Numerical investigation of effective stability and chaos in the J_2–Solar radiation pressure problem

Haris Skokos

Nonlinear Dynamics and Chaos (NDC) group
Department of Mathematics and Applied Mathematics
University of Cape Town, South Africa

E-mail: haris.skokos@uct.ac.za, haris.skokos@gmail.com
URL: http://math_research.uct.ac.za/~hskokos/

International Conference on Nonlinear Science and Complexity (NSC2026)
Thessaloniki, Greece, 15 July 2026

Work supported by the National Research Foundation (NRF) of South Africa
(reference number WABR240401211578)

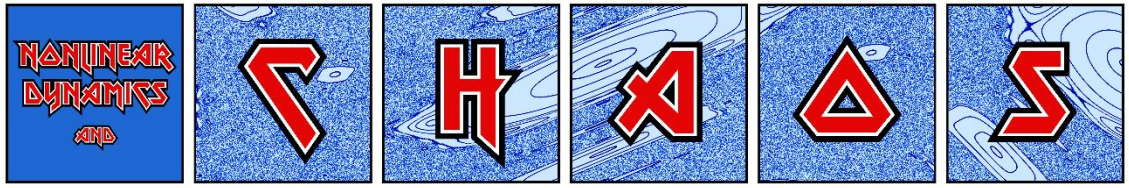

Work in collaboration with

Cassandra Barbis

MSc student, University of Cape Town, South Africa

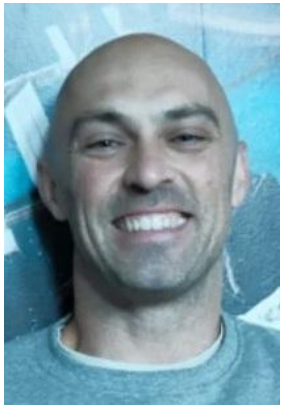

Jérôme Daquin

Centre de Physique Théorique, Luminy Campus, Marseille, France & Université de Toulon, Toulon, France

Elisa Maria Alessi

Istituto di Matematica Applicata e Tecnologie Informatiche "E. Magenes", Milan, Italy

Barbis, Daquin, Alessi & S.: 'Regularity and reentry basins of low Earth orbits in the J_2-solar radiation pressure problem', arXiv:nlin.CD/2605.24575 (2026)

Outline

- Motivation and problem statement:
  In the context of the space debris problem, we extend previous studies by investigating how the coupled effect of solar radiation pressure (SRP) and Earth's oblateness (J_2) can drive chaotic eccentricity growth and enable passive debris reentry.
- Hamiltonian system:
  Perturbations of the two-body problem due to SRP and Earth's oblateness effect.
- Chaos detection:
  The Smaller ALignment Index (SALI).
- Parametric cartography and numerical investigations:
  SALI and orbital lifetime.
- Re-entry basins:
  Smooth and fractal boundaries.
- Summary.

The Hamiltonian model

Hamiltonian model

Following Alessi et al., MNRAS (2018) and Gkolias et al., Celest. Mech. Dyn. Astron. (2020) the motion of a satellite (mass m) around Earth (mass m_E, radius r_E) is described by a perturbed two-body secular Hamiltonian where the Earth's oblateness (J_2) and the solar radiation pressure (SRP) are taken into account:

$$\mathcal{H} = \frac{r_E^2 J_2 \mu^4 (G^2 - 3H^2)}{4G^5 L^3} + n_\odot J - \frac{3 c_R P L^2}{2\mu} \frac{A}{m} \sqrt{1 - \frac{G^2}{L^2}} \sum_{k=1}^{6} \mathcal{T}_k\big(i(L,G,H)\big) \cos\psi_k(g,h,s)$$

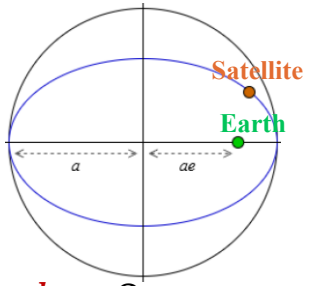

We use Delaunay variables, considering $m \ll m_E$.

$$L = \sqrt{\mathcal{G} m_E a}, \qquad l = M, \qquad G = L\sqrt{1-e^2}, \qquad g = \omega, \qquad H = G\cos i\,, \qquad h = \Omega,$$

related to the orbital elements a (semi-major axis), e (eccentricity), i (inclination), Ω (longitude of node), ω (argument of perigee), and $M(t) = \sqrt{\mathcal{G} m_E} a^{-3/2}(t - t_0)$ (mean anomaly), with $\mathcal{G}$ being the gravitational constant, t is time and t_0 the time at which the satellite is closest to Earth.

$J_2 = 0.0010826$ (oblateness parameter)
$\mu = \mathcal{G} m_E$ (Earth's gravitational parameter)
$c_R = 1$ (reflectivity coefficient)
$P = 4.56 \times 10^{-6}$ (SRP constant at 1 AU)
A/m the area-to-mass ratio
$\varepsilon = 23.4°$(ecliptic's obliquity)
$\lambda_\odot = \lambda_{\odot,0} + n_\odot t$ is the Sun's ecliptic longitude in terms of the Sun's mean motion $n_\odot$

k	$\mathcal{T}_k$	$\cos\psi_k$
1	$\frac{1}{4}(\cos\varepsilon + 1)(\cos i + 1)$	$\cos(\omega + \Omega - \lambda_\odot)$
2	$-\frac{1}{4}(\cos\varepsilon + 1)(\cos i - 1)$	$\cos(-\omega + \Omega - \lambda_\odot)$
3	$\frac{1}{2}\sin i \sin\varepsilon$	$\cos(\omega - \lambda_\odot)$
4	$-\frac{1}{2}\sin i \sin\varepsilon$	$\cos(\omega + \lambda_\odot)$
5	$-\frac{1}{4}(\cos\varepsilon - 1)(\cos i + 1)$	$\cos(\omega + \Omega + \lambda_\odot)$
6	$\frac{1}{4}(\cos\varepsilon - 1)(\cos i - 1)$	$\cos(-\omega + \Omega + \lambda_\odot)$

Note that l is a cyclic coordinate, therefore L and a are constants. We eliminate the system's explicit time dependency due to $\lambda_\odot = \lambda_{\odot,0} + n_\odot t$, by introducing a dummy action variable J conjugate to a variable s such that $s(t) = n_\odot t + \lambda_{\odot,0}$, thereby obtaining an autonomous system with 3 degrees of freedom.

The Smaller ALignment Index (SALI) method of chaos detection

Maximum Lyapunov Exponent (MLE)

Chaos: sensitive dependence on initial conditions.

Roughly speaking, the MLE of a given orbit characterizes the mean exponential rate of divergence of trajectories surrounding it.

Consider an orbit in the *2N*-dimensional phase space with initial condition *x(0)* and an initial deviation vector *v(0)* (small perturbation) from it.
Then the mean exponential rate of divergence is:

$$MLE = \lambda_1 = \lim_{t\to\infty} \Lambda(t) = \lim_{t\to\infty} \frac{1}{t} ln \frac{\|v(t)\|}{\|v(0)\|}$$

$\lambda_1 = 0 \rightarrow$ Regular motion ($\Lambda \propto t^{-1}$)

$\lambda_1 > 0 \rightarrow$ Chaotic motion

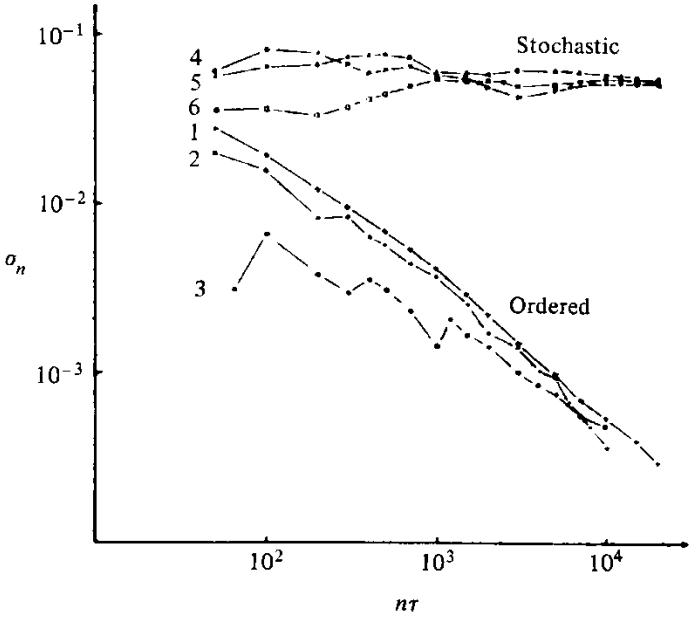

Figure 5.7. Behavior of σ_n at the intermediate energy $E = 0.125$ for initial points taken in the ordered (curves 1–3) or stochastic (curves 4–6) regions (after Benettin *et al.*, 1976).

Definition of the SALI

We follow the evolution in time of two different initial deviation vectors $v_1(0)$, $v_2(0)$ and define SALI [S., J. Phys. A. 34, 10029 (2001) – S. & Manos, Lect. Notes Phys., 915, 129 (2016)] as:

$$SALI(t) = min\{\|\hat{v}_1(t) + \hat{v}_2(t)\|, \|\hat{v}_1(t) - \hat{v}_2(t)\|\}$$

where

$$\hat{v}_1(t) = \frac{v_1(t)}{\|v_1(t)\|}$$

When the two vectors become collinear

$$SALI(t) \rightarrow 0$$

Behavior of the SALI

Hamiltonian flows and multidimensional maps

SALI→0 exponential decay for chaotic orbits

SALI→constant ≠ 0 for regular orbits

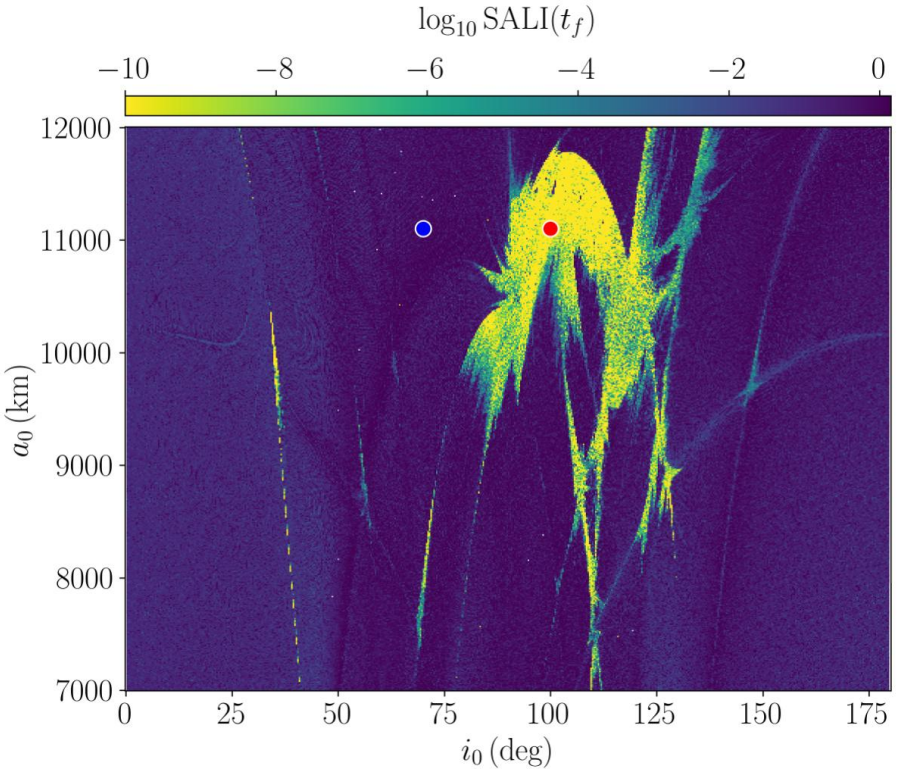

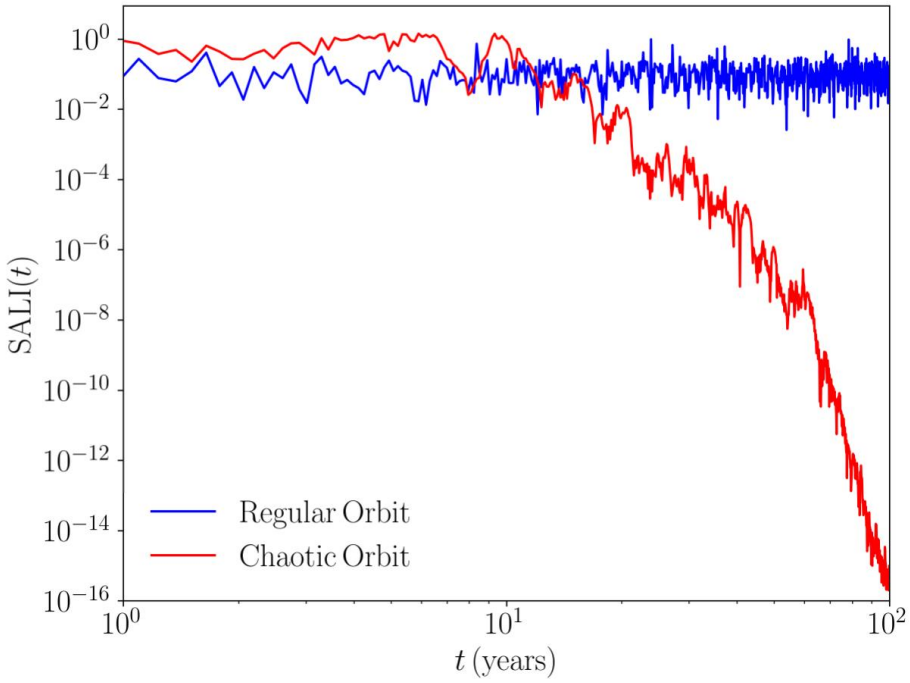

We consider initial conditions (ICs) with $e_0 = 0.05$ and $\omega_0 = \Omega_0 = \lambda_{\odot,0} = 0°$, for $A/m = 10\ \mathrm{m^2 Kg^{-1}}$. We register the SALI at $t_f = 100$ years.

Numerical investigations

Effect of area-to-mass ratio

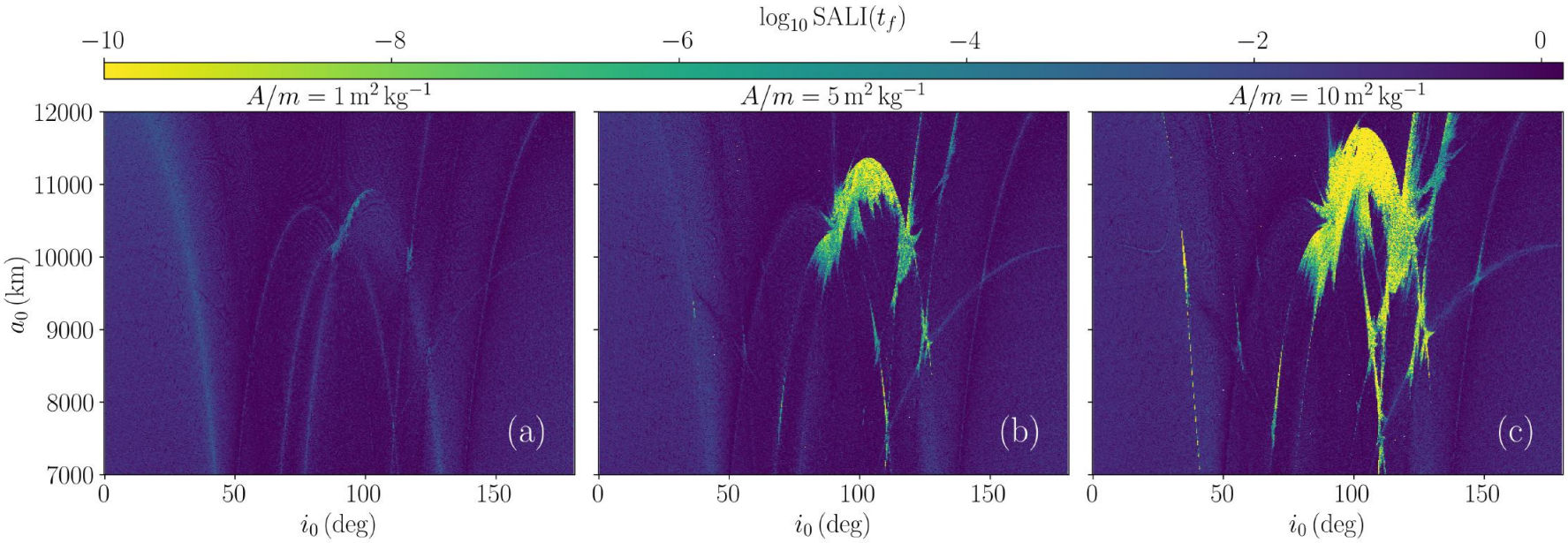

$A/m = 1\ \mathrm{m^2Kg^{-1}}$ $A/m = 5\ \mathrm{m^2Kg^{-1}}$ $A/m = 10\ \mathrm{m^2Kg^{-1}}$

ICs with $e_0 = 0.05$, $\omega_0 = \Omega_0 = \lambda_{\odot,0} = 0°$.
SALI at $t_f = 100$ years.
The extent of chaotic motion increases with increasing A/m values.

Orbital lifetime and re-entry trajectories

Orbital lifetime t_*: the time an orbit with initial semi-major axis a_0 needs to reach the critical eccentricity $e_* = 1 - \frac{r_E+\delta}{a_0}$, [(perigee altitude) $\geq r_E + \delta$] ($\delta = 120$Km and $r_E = 6378.1363$Km). At that time the orbit is considered a re-entry trajectory.

The majority of re-entry orbits are associated with re-entry times shorter than 5 years.

$$N_* \sim t_*^{-2}$$

N_*: the number of ICs (out of about 260,000 considered orbits) leading to re-entry for times less than 25 years.

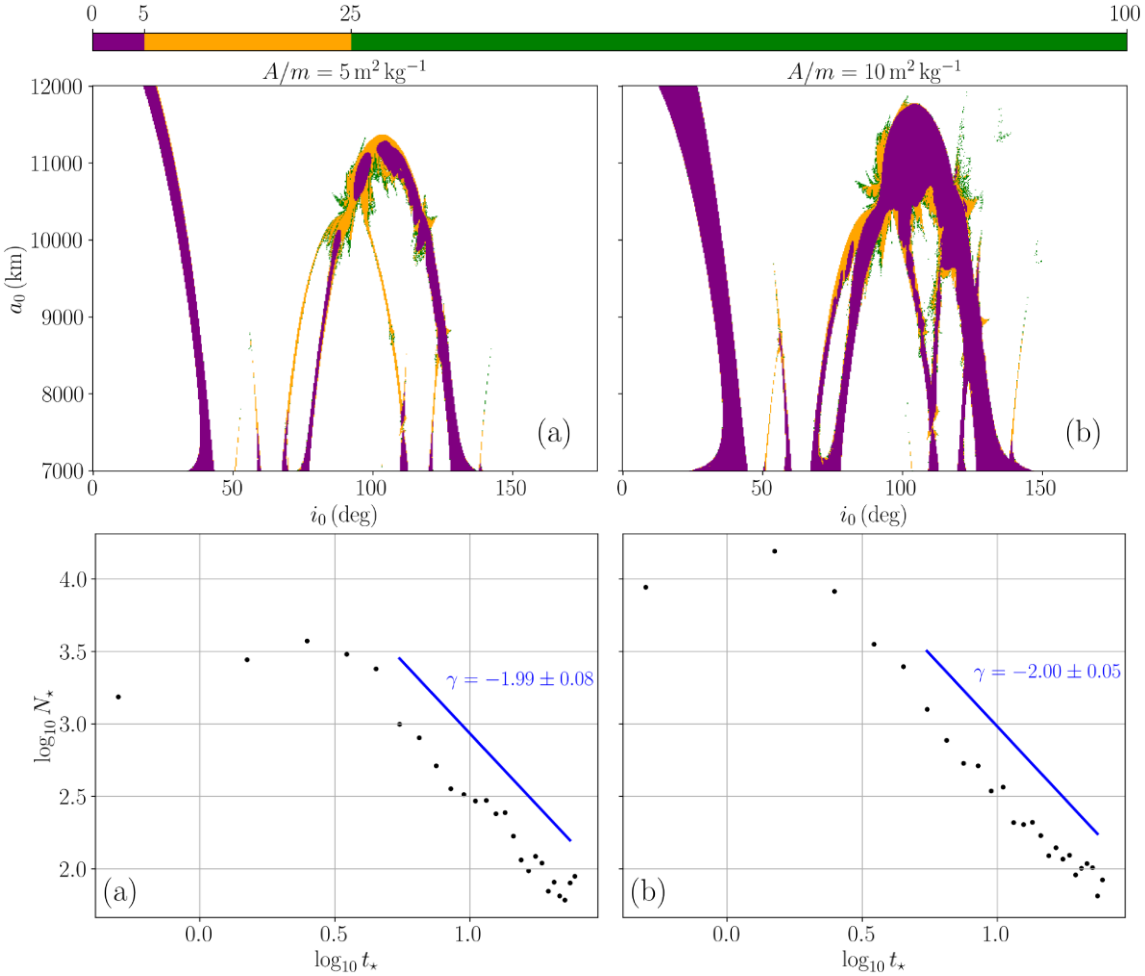

Chaoticity and orbital lifetimes

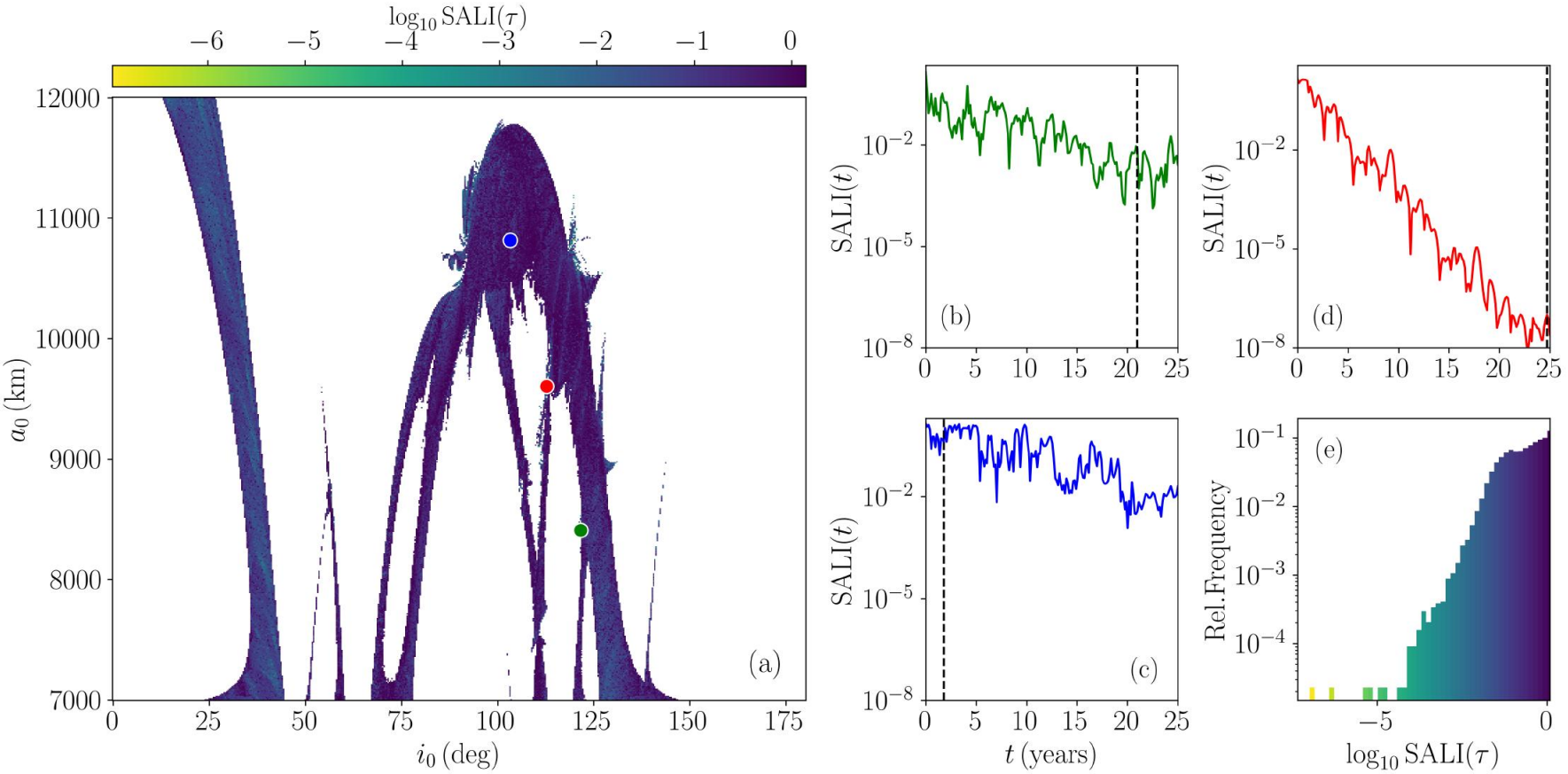

SALI is computed at the effective time τ, which is the orbital lifetime t_* of orbits with $t_* \leq 25$ years.

Almost all re-entry orbits exhibit regular behavior until the time of re-entry.

Chaoticity and orbital lifetimes

Orbits with $t_* \leq 100$ years.

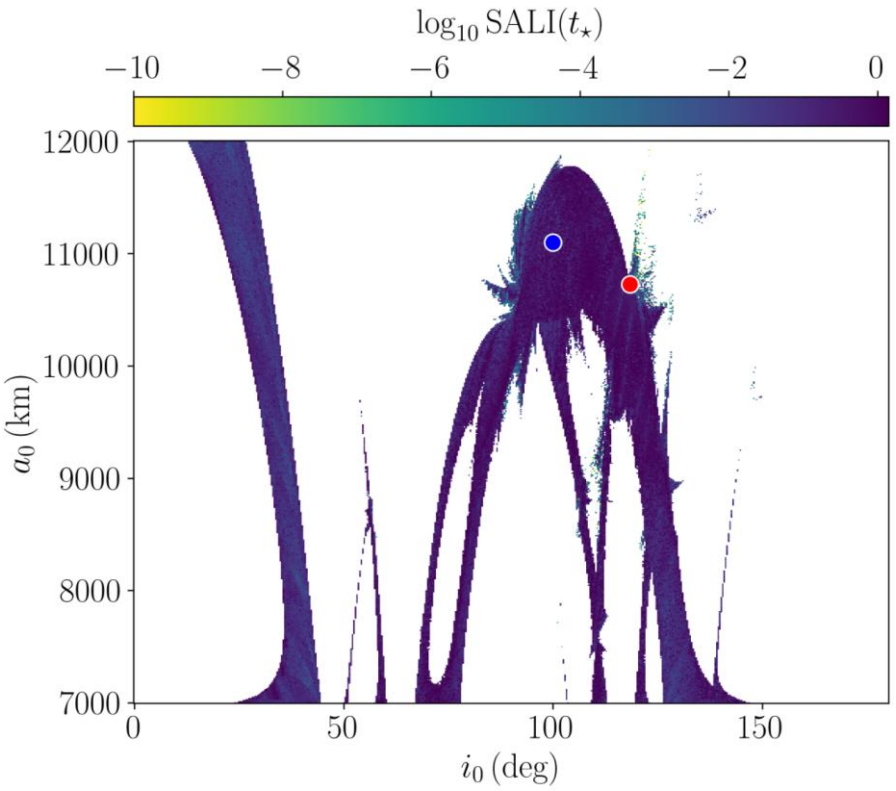

$(a, e, i, \omega, \Omega) = (11100\text{Km}, 0.05, 100°, 0°, 0°)$

$(a, e, i, \omega, \Omega) = (10727.98\text{Km}, 0.05, 118.36°, 0°, 0°)$

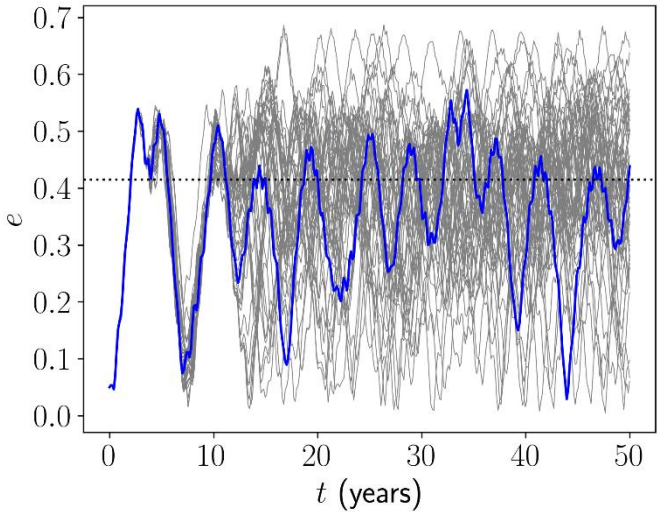

e_*

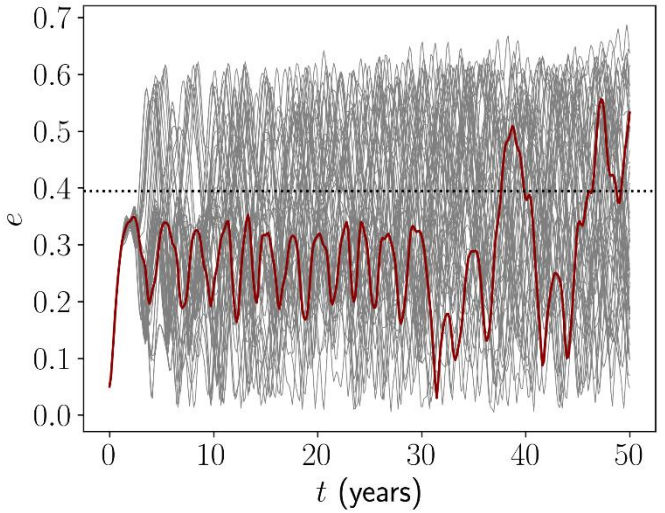

e_*

We consider 50 randomly generated ICs (grey curves) within the neighborhood of the nominal orbit.

Re-entry basins

We set $A/m = 10\ \mathrm{m^2 Kg^{-1}}$ and consider sets of re-entry points following the 5-year and 25-year mitigation scenario.

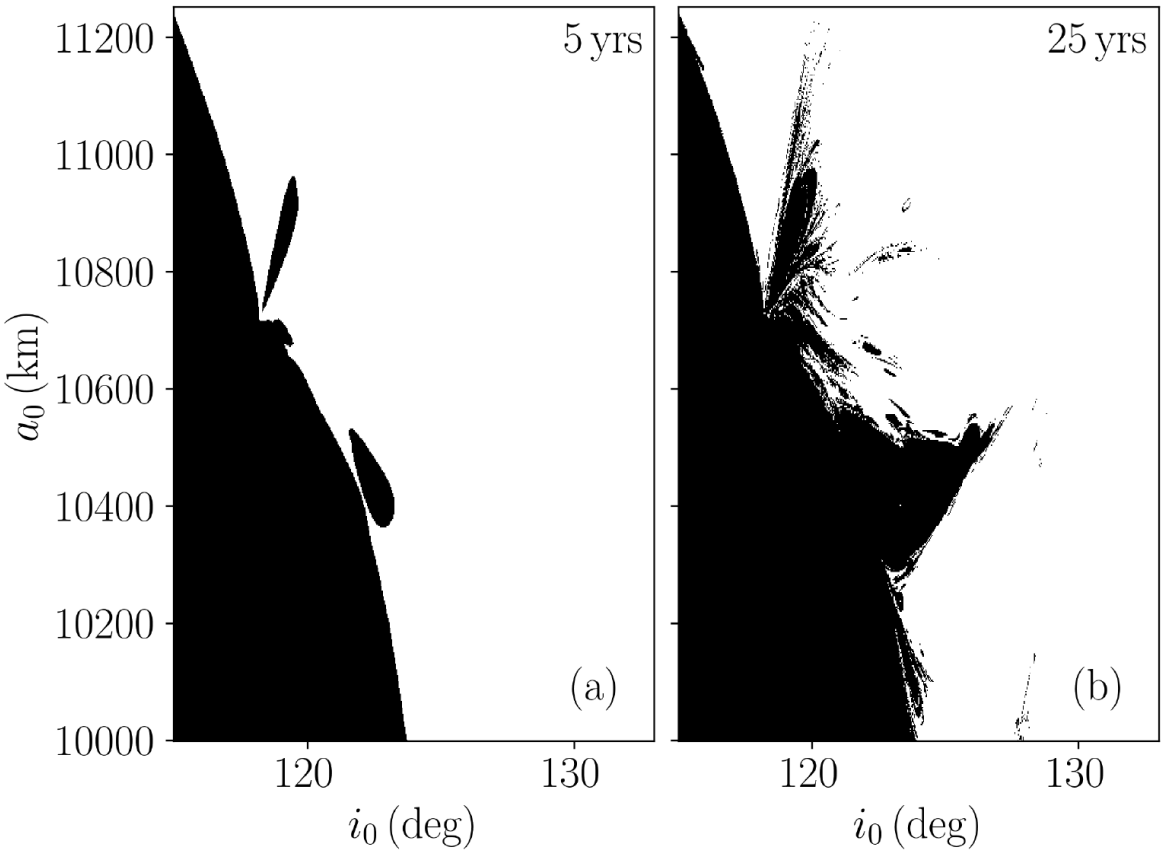

Basin boundaries look fractal for the less-stringent mitigation scenario.

Uncertain points and uncertainty exponent

Following Grebogi et. al., Phys. Lett. A, 99, 415 (1983) an IC $\boldsymbol{x_0}$ is ϵ-uncertain if two nearby ICs $\boldsymbol{x_0} \pm \epsilon$ (we perturb only the inclination i by ϵ) do not show the same behavior with respect to the considered mitigation scenario.

$N_u(\epsilon)$: number of ϵ-uncertain ICs, N: number of considered ICs
$f(\epsilon)$: uncertainty fraction, α: uncertainty exponent

$$f(\epsilon) = \frac{N_u(\epsilon)}{N} \propto \epsilon^{\alpha}$$

$\alpha = 1$: Smooth boundaries
$0 < \alpha < 1$: Fractal boundaries.
A substantial improvement in the IC uncertainty ϵ, yields only a relative small decrease in the uncertainty of the final state as measured by f.
Example: For $\alpha = 0.5$ reducing the uncertainty in the ICs by a factor of 100 decreases the fraction of uncertain points by only a factor of 10.

Uncertain points and uncertainty exponent

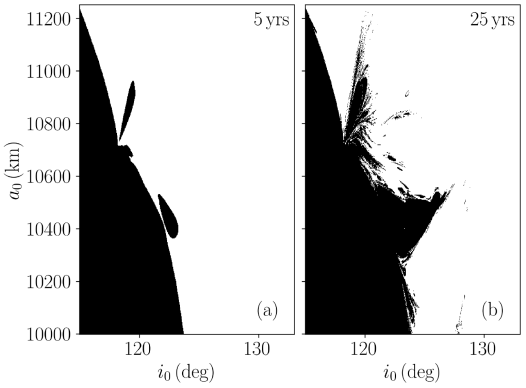

The set of uncertain points develops a significantly more intricate structure for less-stringent mitigation scenarios.

Uncertain points for $\epsilon \approx 0.034°$

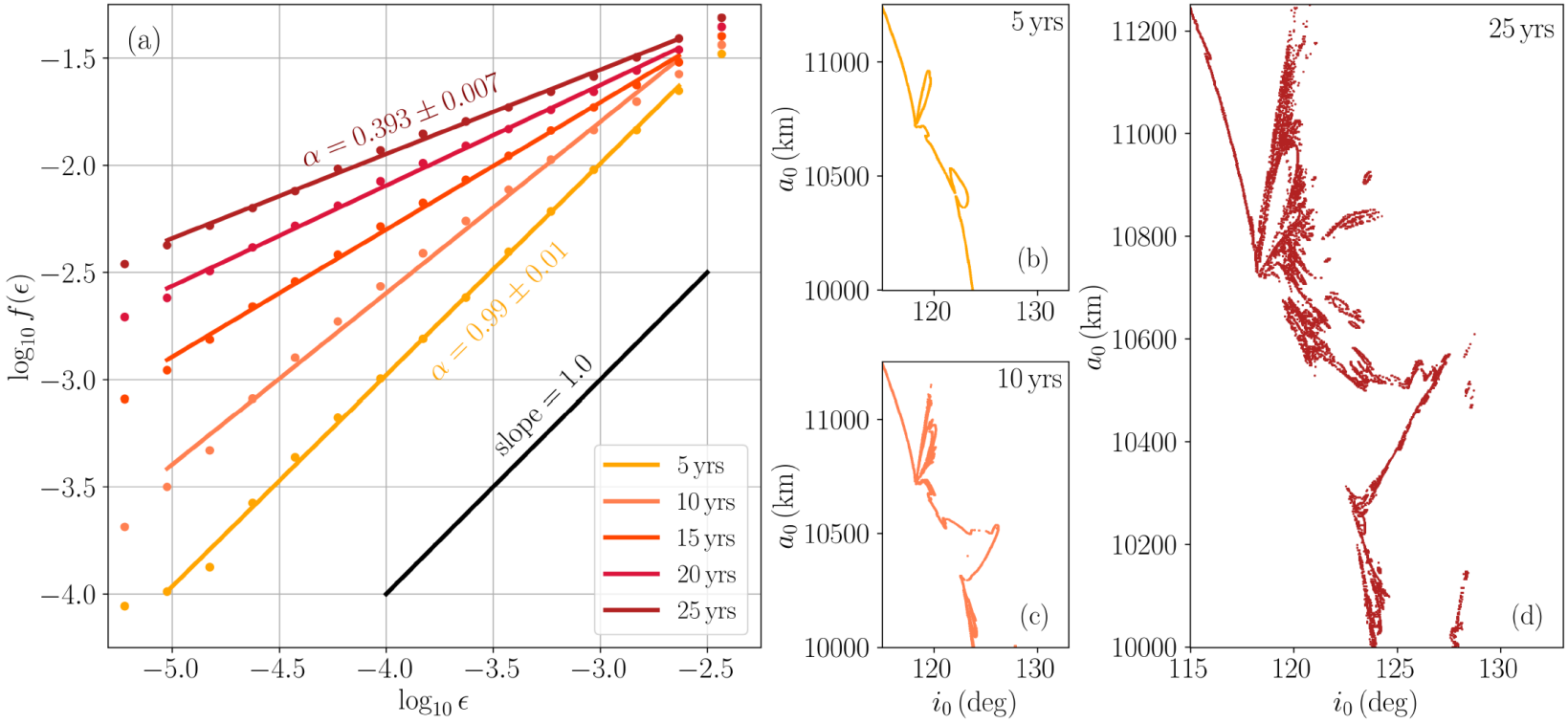

Uncertain points and uncertainty exponent

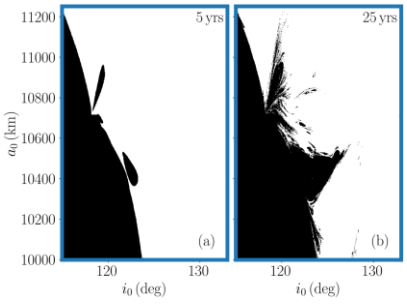

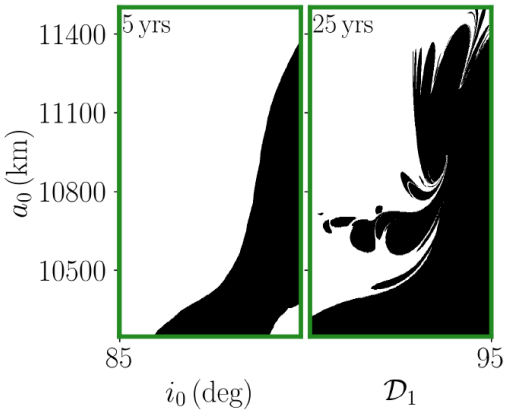

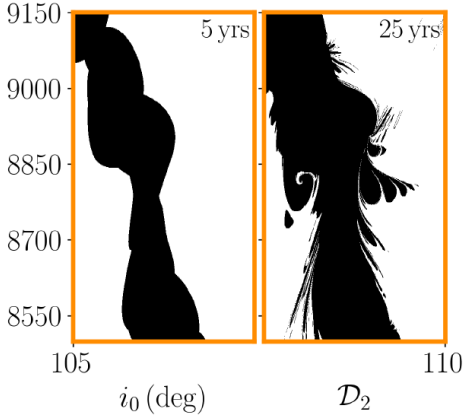

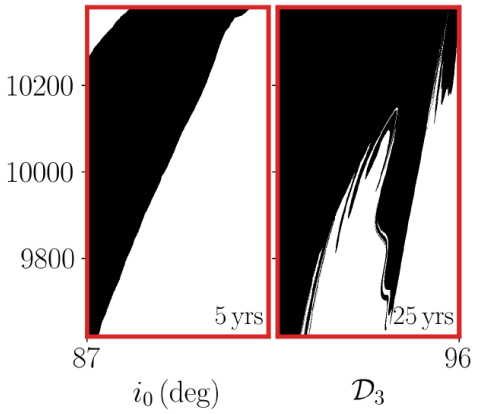

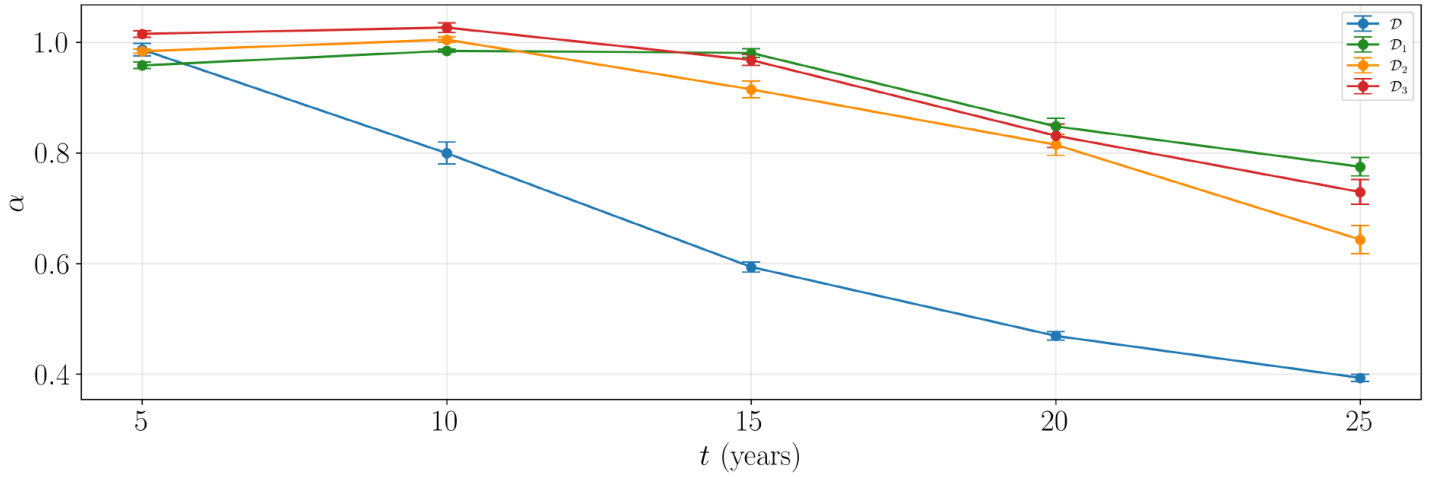

The value of the uncertainty exponent α decreases (fractality increases) for less-stringent mitigation scenarios.

Summary

- We conducted a numerical investigation of Earth satellite orbital dynamics under perturbations to the two-body Kepler problem arising from solar radiation pressure and the Earth's oblateness.
- The Smaller ALignment Index method (SALI) allows the fast and clear identification of chaotic regions.
- The extent of chaos increases with increasing A/m values.
- The number N_* of re-entry trajectories follows a power law decay with respect to the orbital lifetime t_*: $N_* \sim \frac{1}{t_*^2}$.
- Almost all re-entry trajectories with $t_* \leq 25$ years exhibit regular behavior until the time of re-entry.
- Boundaries of re-entry basins become increasingly fractal (lower uncertainty exponent) as the mitigation timescale increases from 5 to 25 years.
- From an operational perspective targeting the 5-year re-entry basin is easier than targeting the 25-year basin.